Electrochimica Acta 335 (2020) 135432

Contents lists available at ScienceDirect

Electrochimica Acta

journal homepage: www.elsevier.com/locate/electacta

Solution phase superoxide as an intermediate in the oxygen reduction reaction on glassy carbon in alkaline media

Jonathan R. Strobl, Nicholas S. Georgescu, Daniel Scherson*

Department of Chemistry, Case Western Reserve University, Cleveland, OH, 44106-7078, USA

ARTICLE INFO

Article history:
Received 1 November 2019
Received in revised form
27 November 2019
Accepted 1 December 2019
Available online 5 December 2019

Keywords:
Oxygen reduction
Electrocatalysis
Glassy carbon electrode

ABSTRACT

A 3-mercapto-1-propanol (3M1P)-modified Au ring electrode has been employed to monitor solution phase superoxide, O_2^-(aq), generated at the surface of a glassy carbon (GC) disk of a ring-disk rotating electrode (RRDE) in 0.1 M NaOH aqueous solutions. Measurements performed at various rotation rates afforded unambiguous evidence that maximum yields for O_2^-(aq) is attained at potentials associated with a current minimum in the polarization curve at $E_{disk} = 0.3$ V vs RHE, with a ca. 18% faradaic efficiency. In stark contrast, no O_2^-(aq) could be detected in virtually identical experiments involving Au and Pt disk electrodes. This finding indicates that, if superoxide is involved in the mechanism of O_2(aq) reduction on these metals, it remains adsorbed on the surface and is subsequently reduced, or, if desorbed, the rate of its reduction would be high enough for its concentration to decrease to undetectable levels at the functionalized Au-ring under the experimental conditions employed.

1. Introduction

The oxygen reduction reaction (ORR) on carbonaceous surfaces in alkaline aqueous media has been the subject of considerable attention in the electrochemical literature for several decades [1–3], owed, by and large, to the continuing development of noble metal free alkaline fuel cells, and the large scale synthesis of hydrogen peroxide. Based on data reported by numerous laboratories, including cyclic voltammetry in stagnant solutions, and dynamic polarization using a rotating disk, RDE, and ring-disk electrode, RRDE, techniques, for a variety of carbon materials, including glassy carbon, GC, and ordinary pyrolytic graphite, OPG, the ORR in basic electrolytes proceeds predominantly via a 2-electron process to yield solution phase peroxide, HO_2^-(aq) [1–4]. Additional evidence in support of this view was obtained from Koutecky-Levich analyses of RDE data recorded at various rotation rates, which yielded a value of n, the net number of electron transferred in the process, of 2.1 ± 0.1 [2]. An intriguing aspect of this reaction is the presence of a current minimum in polarization curves recorded with the RDE (see, for example, Fig. 5 in Ref. 1). Various authors have attributed this peculiar effect to changes in the oxidation state of functional groups present on the carbon surface, which modulate the overall activity of the electrode as a function of the applied potential [2,3,5]. In fact, intentional modification of the GC surface involving covalent attachment of species, such as quinones, which are known to undergo redox reactions in the potential range where this phenomenon is found, have led to the disappearance of the minimum, to yield polarization curves characterized by a shoulder for small overpotentials (see, for example, Fig. 5 in Ref. 3). From a mechanistic viewpoint, the pathways proposed for ORR on polished carbon electrodes in alkaline solutions, have considered only adsorbed species [1,2,4,6], including dioxygen, superoxide, and peroxide, as possible intermediates, and HO_2^-(aq) (and to a far less extent, OH^-(aq)), as the predominant product (see, e.g. Fig. 7 in Ref. 1). A notable exception, is that of the work by Xu et al.[6], who suggested generation of solution phase superoxide, O_2^-(aq), to account for the presence of a very small oxidation peak found upon reversing the voltammetric scan following reduction of O_2(aq) in quiescent tetraethyl ammonium hydroxide aqueous solutions, (see Fig. 7, Ref, 4), a feature that was totally absent in alkali metal hydroxides electrolytes. It should be emphasized, that 4-methylbenzene functionalized GC surfaces [3,6], did display a highly reversible redox process attributed by these authors to the O_2/O_2^-(aq) couple.

This contribution describes the use of a 3-mercapto-1-propanol (3M1P)- functionalized Au ring electrode that exhibits extraordinary specificity for the oxidation of solution phase superoxide, O_2^-(aq), and is virtually impervious to the presence of HO_2^-(aq), to

* Corresponding author.
E-mail address: dxs16@case.edu (D. Scherson).

https://doi.org/10.1016/j.electacta.2019.135432
0013-4686/

explore more detailed mechanistic aspects of the ORR in 0.1 M NaOH, on GC, as well as other electrode materials. A preliminary report describing the virtues of this functionalized Au ring electrode was recently published in our laboratory for neutral aqueous solutions [7]. As will be shown, the minimum found in polarization curves collected with the RDE technique referred to above, is associated with a change in the mechanism of the ORR induced by a yet to be identified surface process, that promotes production of O_2^-(aq), thereby reducing the observed diffusion limited current over a relatively narrow potential range.

2. Experimental section

All measurements were performed in 0.1 M NaOH electrolyte prepared by adding solid NaOH (Honeywell, Semiconductor Grade, 99.99% metals basis) to ultrapure water (UPW) from a Barnstead NANOpure DIamond™ water purification system. Hydrogen peroxide (Fisher, 30%, Certified ACS) was used as received. All cell components were composed of either glass or Teflon, and cleaned by soaking overnight in piranha solution (10:1 concentrated H_2SO_4 [Fisher, Certified ACS Plus] to 30% aqueous H_2O_2) followed by alternatively rinsing and boiling in UPW (4 times each). ***NOTE: Piranha solution is highly corrosive and oxidizing. Care must be taken when preparing and handling this solution.*** Experiments were carried out by saturating the electrolyte with oxygen (Airgas, 99.999%), which was bubbled through the electrolyte for a minimum of 10 min, or until the currents for ORR became time independent. A graphite rod and a home-made hydrogen bubble reversible hydrogen electrode (RHE)[8], were used as counter and reference electrodes, respectively. Measurements were performed with a Pine ChangeDisk Au|Au rotating ring-disk electrode, RRDE, which was rotated with a Pine Analytical Rotator driven by a Pine MSRX Speed Controller. The ring and disk potentials were controlled by a Pine RDE 3 potentiostat. The RRDE (Au|GC, Au|Au or Au|Pt) was cleaned by first demounting the disk and then polishing the ring and disk electrodes on separate polishing cloths (Buehler) with 1, 0.25 and 0.05 μm diamond powder (Buehler) to prevent cross contamination. The electrode was then rinsed with UPW water and sonicated in the same media for 5 min. The 3-mercapto-1-propanol (3M1P)-modified Au ring electrode was prepared by the method described by Feng et al. [7] by first removing the GC disk from the demountable Au|GC RRDE assembly and replacing it with a Teflon insert, which was subsequently immersed into a 10 mM solution of 3M1P (Aldrich, 95%) in ethanol (Decon Laboratories Inc, 200 proof) for a minimum of 16 h. Following copious rinsing with UPW, the Teflon insert was replaced by the GC disk.

3. Results and discussion

3.1. Specificity of 3M1P-functionalized Au toward the oxidation of solution-phase superoxide in pH 13 aqueous solutions

Clear evidence of the ability of 3M1P-functionalized Au to selectively oxidize O_2^-(aq) in 0.1 M NaOH solutions containing HO_2^-(aq), was provided by monitoring the current flowing through the ring of a Au^{3M1P}|GC RRDE, i_{ring}^{3M1P}, polarized at E_{ring} = 0.9 V (black) and E_{ring} = 1.0 V (red) as a function of time in the O_2-saturated based electrolyte (see Fig. 1). For these experiments, the RRDE was rotated at ω = 900 rpm, while the disk potential, E_{disk}, was fixed at 0.2 V vs RHE. As shown by the dynamic polarization curve for the GC disk recorded at 0.02 V/s in the same electrolyte (see Insert), O_2(aq) reduction at this potential proceeds at substantial rates. The black and red symbols in the Insert, represent, respectively, steady state i_{disk} values for E_{disk} = 0.2 V, i.e. close to the minimum, for E_{ring} = 1.0 V (black symbol) and E_{ring} = 0.9 V (red symbol), collected in fully independent experiments. In fact, the

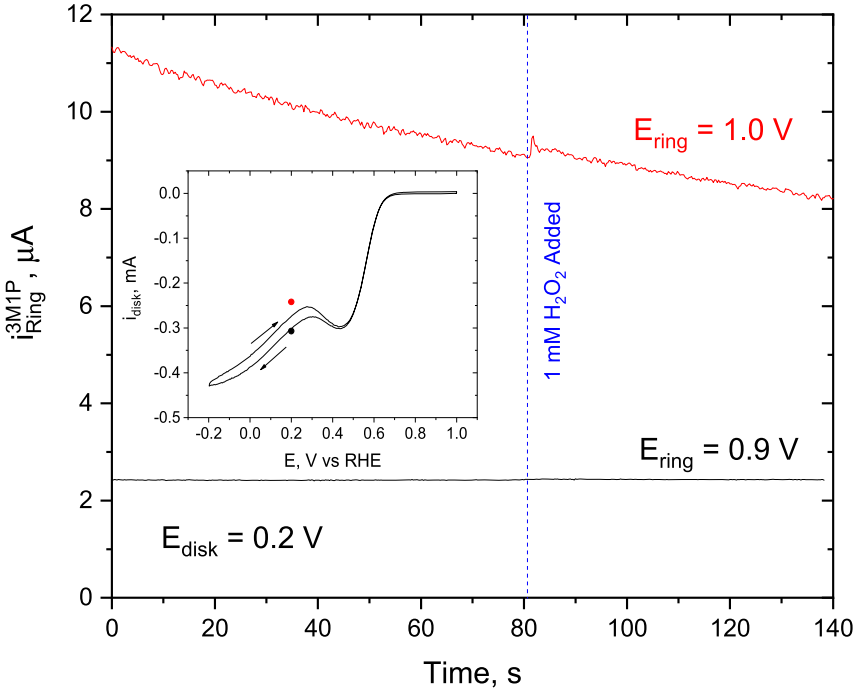

Fig. 1. Plots of i_{ring}^{3M1P} vs time recorded with the functionalized Au ring of a Au^{3M1P}|GC RRDE rotating at ω = 900 rpm polarized at E_{ring} = 0.9 V (black) and E_{ring} = 1.0 V (red) as a function of time in O_2-saturated 0.1 M NaOH, while E_{disk} was fixed at 0.2 V vs RHE. The vertical blue line indicates the time at which H_2O_2 was added to the solution to a concentration of 1 mM. **Insert:** Dynamic polarization curve for the GC disk recorded at 0.02 V/s in the same electrolyte, where the black and red symbols represent steady state i_{disk} values for E_{disk} = 0.2 V vs RHE, for E_{ring} = 1.0 V (black symbol) and E_{ring} = 0.9 V (red symbol) collected in fully independent experiments. (For interpretation of the references to color in this figure legend, the reader is referred to the Web version of this article.)

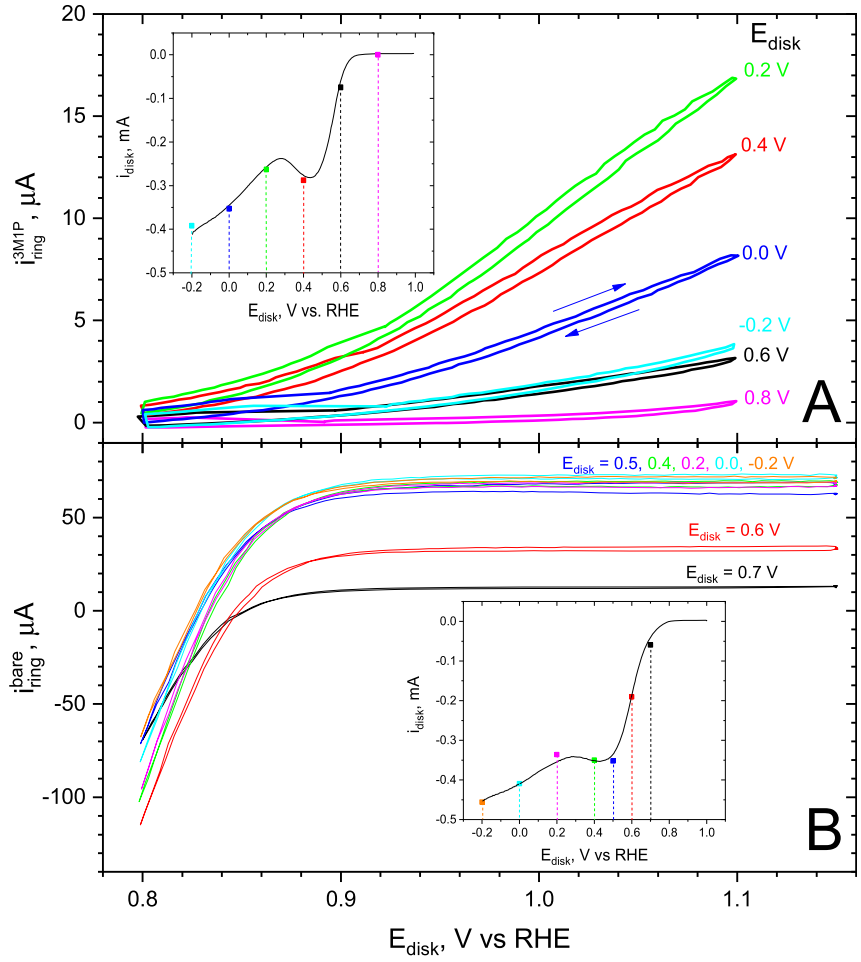

Fig. 2. Panel A. Dynamic polarization curves ($\nu = 20$ mV/s) recorded with the Au_{ring}^{3M1P} of a Au|GC RRDE in O_2-saturated 0.1 M NaOH at $\omega = 900$ rpm, while the GC disk was polarized at the values specified in the figure. **Panel B**. Same as Panel A, for a pristine (non-functionalized) Au ring electrode. **Inserts:** Dynamic polarization curve ($\nu = 20$ mV/s) collected with the GC disk recorded toward positive potentials, under the same conditions, where the different colored symbols represent steady-state disk currents measured while collecting the ring polarization curves in the main panel.

difference in the actual magnitudes of i_{disk} illustrate the high sensitivity of the minimum to perhaps minute changes in the GC surface preparation. As clearly indicated in Fig. 1 (see black curve), no changes in i_{ring}^{3M1P} could be detected upon introducing H_2O_2 to the solution to a concentration of 1 mM (see blue vertical line) for $E_{ring} = 0.9$ V. Analogously, no changes in the rate at which i_{ring}^{3M1P} decreased over time were observed following H_2O_2 addition for $E_{ring} = 1.0$ V (see red curve), affording clear evidence that, under the specified experimental conditions, the Au_{ring}^{3M1P} is only active toward O_2^-(aq) oxidation and impervious to the presence of HO_2^-(aq) in solution. It should be emphasized that identical experiments in which the solution was purged with N_2(gas) yielded no detectable ring currents. Shown in the upper panel, Fig. 2 is a set of dynamic polarization curves recorded with the Au_{ring}^{3M1P} ring of a Au|GC RRDE in O_2-saturated 0.1 M NaOH at $\nu = 20$ mV/s, and $\omega = 900$ rpm, while the disk $E_{disk}$was polarized at $E_{disk} = 0.2$ V (see colored symbols in the Insert). Also displayed in the Insert are dynamic polarization curve for the GC disk recorded at $\nu = 0.02$ V/s in the same electrolyte. As indicated, all currents showed a monotonic increase as the potential was scanned toward positive values, regardless of E_{disk}. Moreover, i_{ring}^{3M1P} displayed very small hysteresis, which suggests that the ring activity is not affected within the time scale of the voltammetric measurements.

A markedly different behavior was found for identical experiments involving a pristine, i.e. non-functionalized, Au ring, for which the currents were much higher than those found for the functionalized counterpart (see Lower Panel, Fig. 2), and relatively constant for $E_{ring} > 0.9$ V, signaling that the bare Au ring is in all likelihood capturing both O_2^-(aq) and HO_2^-(aq) under diffusion limited control. It has been argued [2], that since i_{ring}/i_{disk} is very close to N for a bare Au ring, as the experimental data strongly indicates, polished GC would generate HO_2^-(aq) with ca. 100% efficiency. This is, however, not the case, as the ratio would still be N, even if the reaction would proceed via a one electrode pathway to yield O_2^-(aq). Lastly, the fact that i_{ring}^{bare} reversed sign for $E_{ring} < 0.9$ V, is to be expected for the ORR on bare Au in this electrolyte (see Fig. 5, below).

Although the fact that i_{ring}^{3M1P} did not reach a plateau characteristic of a diffusion limited current will prevent a full quantitative analysis of the data collected, highly valuable information regarding the mechanism of ORR as a function of the applied potential could be gleaned from RRDE measurements involving a Au_{ring}^{3M1P}|GC RRDE (see Fig. 3) polarization curves recorded for

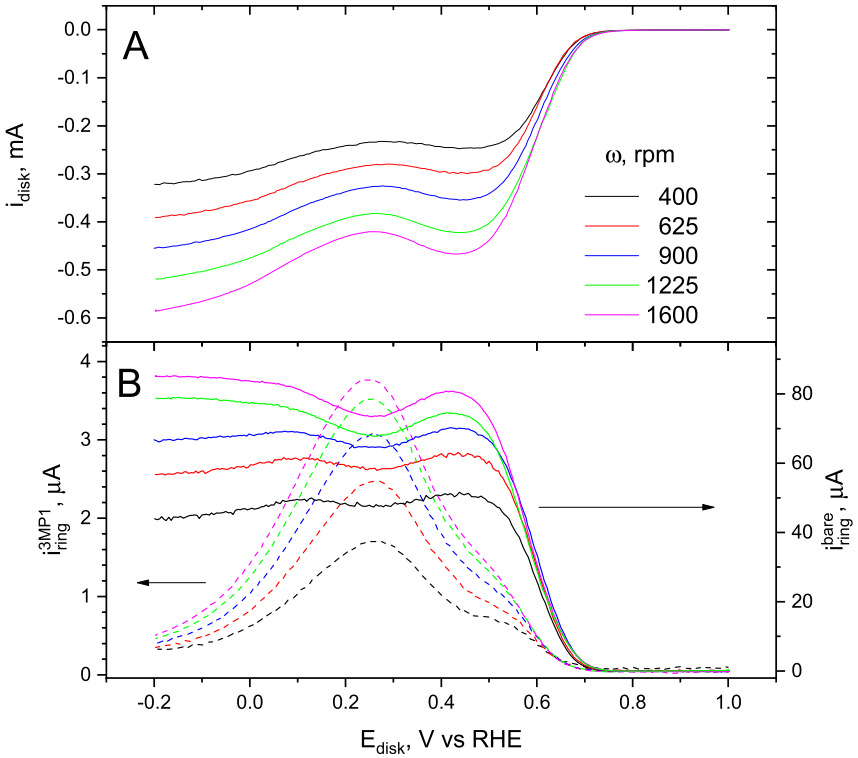

Fig. 3. Panel A. Dynamic polarization curves (20 mV/s) collected for a polished GC disk electrode of a Au|GC RRDE in O_2-saturated 0.1 M NaOH at rotation rates, ω, in the range 400−1600 rpm, as indicated. **Panel B.** Corresponding currents recorded simultaneously with either a 3MP1-modified Au ring electrode polarized at 0.9 V, i^{3M1P}_{ring} (dashed lines, left axis) or a bare Au ring electrode, i^{bare}_{ring} (solid lines, right axis), polarized at E_{ring} = 1.15 V.

several rotation rates. The results of these experiments are summarized in the next section.

3.2. Mechanistic studies of ORR using a Au|GC RRDE

In agreement with data reported in the literature (see, for example, Fig. 3 in Ref. 1), dynamic polarization curves (ν = 20 mV/s) for a polished GC disk of a Au|GC RRDE recorded in O_2-saturated 0.1 M NaOH, yielded for rotation rates, ω, in the range 400 < ω < 1600 rpm, a bare Au ring response at E_{ring} = 1.15 V, which virtually mirrored that obtained with the GC disk (see solid lines, right ordinate, Fig. 3) for all ω values. Also shown in dotted lines in the lower panel in this figure is the response of the Au^{3M1P}_{ring} in otherwise identical experiments, which, unlike that of the bare Au ring, displayed a bell shape character reaching a maximum precisely at the potential at which the minimum was observed for the GC disk (and the corresponding response of the bare Au ring). It may be concluded, based on these results, that the minimum in the polarization curves signals a change in the ORR mechanism, whereby a significant fraction of the disk current can be attributed to a one-electron reduction of O_2(aq), to yield O_2^-(aq), for which the standard redox potential is ca. −0.33 V vs SHE [3]. To the best of our knowledge, this is the first time direct evidence has been obtained for this latter species being involved in the ORR on polished GC. As was mentioned above, this behavior is to be contrasted with that displayed by GC electrodes functionalized by a variety of redox active species, as illustrated by the work on McCreery and coworkers for methyl-phenyl adlayers [3], who did detect O_2^-(aq). On this basis, it seems reasonable to assume that groups of this type are also present in polished GC, and presumably in other carbonaceous materials.

3.3. Faradaic efficiencies for solution phase superoxide formation during ORR on glassy carbon electrodes

Estimates of the minimum amount of O_2^-(aq) generated at the GC electrode under the conditions selected for this study, were obtained from measurements in which E_{disk} was held at a given value until a steady current was achieved, while the ring was set at E_{ring} = 0.9 V. Subsequently, E_{ring} was stepped to 1 V for a time t < 3 s, and then stepped back to 0.9 V, in order to minimize the amount of time spent at the higher potential and, therefore, mitigate problems associated with the decay of i_{ring} over time (Fig. 1). As shown in Appendix I, the rate of homogeneous dismutation of $O_2^-(aq)$ is too small to influence the ring current at this pH. Hence, the steady state ring currents recorded at 1.0 V, shown in Panel B, Fig. 4, which are approximately 4 times larger than those measured at 0.9 V (see e.g. Panel A, Fig. 2), can be used to calculate a ***minimum*** amount of O_2^-(aq) produced at the disk, by assuming (incorrectly) that $O_2^-(aq)$ oxidation on the functionalized Au ring proceeds under diffusion limited conditions. This quantity can be expressed as a minimum faradaic yield, $Y^{min}_{O_2^-}$, as follows:

$$Y^{min}_{O_2^-} = \frac{i^{3M1P}_{ring}}{N \cdot i_{disk}} \quad (1)$$

These values are shown in Panel B, Fig. 4, from which the minimum value of $Y^{min}_{O_2^-}$ was found to be ca. 18% at E_{disk} = 0.3 V vs RHE.

3.4. Comparison with other common electrode materials

Shown in Panel A, Fig. 5 are polarization curves for GC, Au and Pt in O_2-saturated 0.1 M NaOH at 900 rpm and the corresponding ring

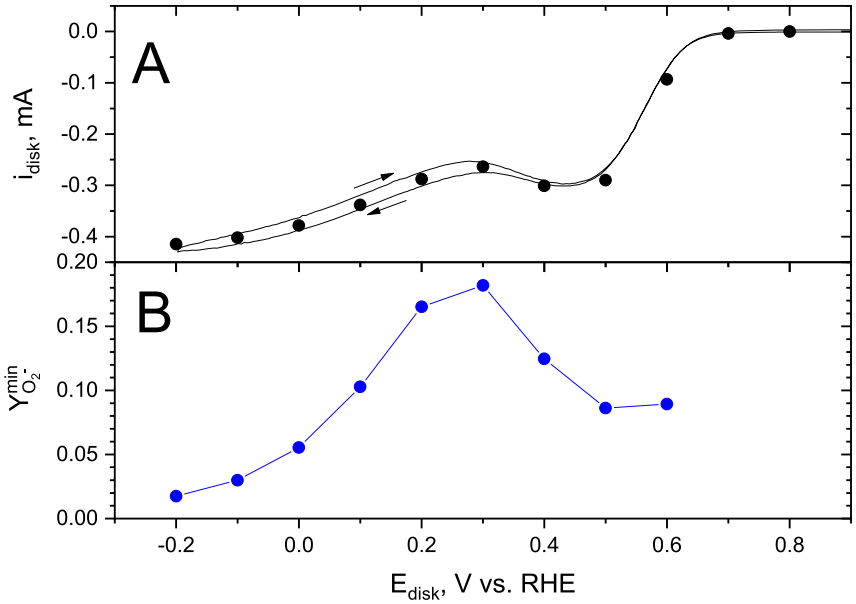

Fig. 4. Panel A. Dynamic polarization curves (ν = 20 mV/s) recorded with a GC disk electrode rotating at ω = 900 rpm in O_2-saturated 0.1 M NaOH. The solid symbols represent measurements performed while the GC disk was polarized at the specified potentials for ca. 5 s. (see text for details). **Panel B.** Plot of $Y^{min}_{O_2}$ vs E_{disk} based on i^{3M1P}_{ring} measured at 1 V and Eq. (1).

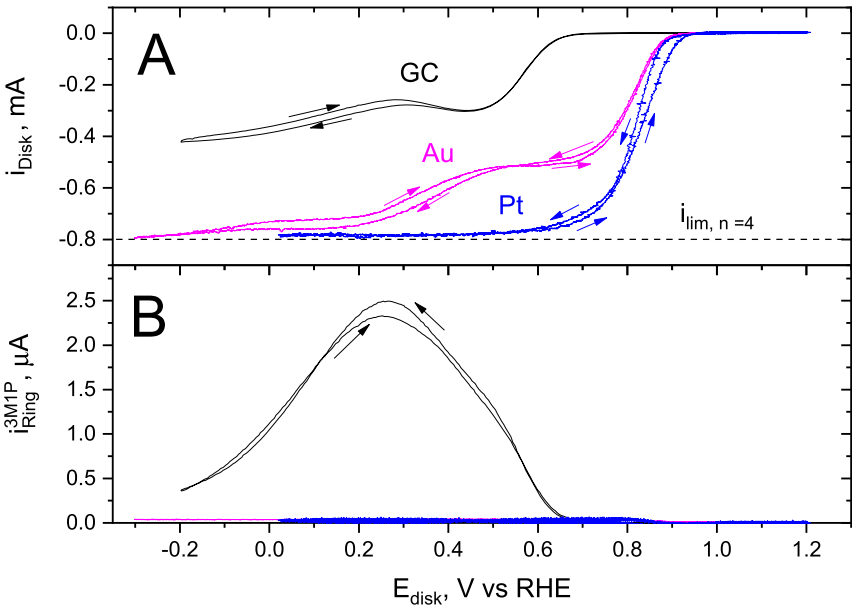

Fig. 5. Panel A. Polarization curves collected in O_2-saturated 0.1 M NaOH at 20 mV/s and 900 rpm for GC, Au and Pt disk as specified. **Panel B**. Ring currents collected with a concentric 3M1P-modified Au ring polarized at E_{ring} = 0.9 V, while the disk currents were recorded.

currents for a 3M1P-modified Au ring electrode (see Panel B in this figure). As clearly indicated, no ring currents could be detected for either metal. Not surprisingly, no disk or ring currents could be detected for any of the electrodes examined in N_2 purged solutions (not shown). In fact, Zurilla et al. invoked theoretical arguments to exclude the possibility of $O_2^-(aq)$ as being a possible intermediate for ORR on Au at pH 13 [5]. However, $O_2^-(aq)$ has been claimed to be an intermediate for this reaction on Pt in far more concentrated alkaline solution based on scanning electrochemical microscopy studies reported by Zhang et al. [9].

Summary

Rotating ring-disk measurements using a 3-mercapto-1-propanol (3M1P)-modified Au ring electrode have provided evidence that the minimum found in polarization curves for oxygen reduction reaction on a polished glassy carbon disk in 0.1 M NaOH is associated with generation of solution phase superoxide, O_2^-(aq), over a wide potential range. Quantitative estimates have indicated that the amount of O_2^-(aq) produced can reach values of at least 18%. In contrast, no O_2^-(aq) could be detected when using Pt or Au

disk electrodes in agreement with earlier claims made in the literature.

Author Contributions

Jonathan Strobl performed all the experiments and contributed to the analysis of the data. Nicholas Georgescu was responsible for much of the data analysis including the COMSOL simulations. Daniel Scherson originated many of the ideas and supervised the work.

Acknowledgements

This work was supported by NSF CHE-1808592.

Appendix I. On the effects of solution phase superoxide dismutation on measurements of the oxygen reduction reaction in pH 13 aqueous solutions using rotating ring-disk electrodes

The primary objective of this Appendix is to show that under the conditions selected for our studies, the dismutation of solution phase superoxide, O_2^-(aq), proceeds at negligible rates and therefore its effect on the response of the ring electrode can be safely ignored. In their classic paper, Bielski and coworkers [11] showed that at least one protonated superoxide species is required to drive its dismutation at measurable rates, i.e.

Table A.1
Governing Differential Equations and Boundary Conditions

$$\nabla^2 P - U\cdot\nabla P + \frac{1}{2}\alpha Q^2 = 0 \quad \text{(A1)}$$

$$\chi\nabla^2 Q - U\cdot\nabla Q - \alpha Q^2 = 0 \quad \text{(A2)}$$

$$U_R = 3RZ, \quad U_Z = 3Z^2 \quad \text{(A3)}$$

$$P_{Z=3\Delta} = 1 \quad \text{(A4)}$$

$$Q_{Z=3\Delta} = 0 \quad \text{(A5)}$$

$$P_{Z=0,R<R_1} = 0 \quad \text{(A6)}$$

$$\left.\frac{dP}{dZ}\right|_{Z=0,R<R_1} + \chi\left.\frac{dQ}{dZ}\right|_{Z=0,R<R_1} = 0 \quad \text{(A7)}$$

$$Q_{Z=0,R_2<R<R_3} = 0 \quad \text{(A8)}$$

$$2HO_2(aq) \rightarrow O_2(aq) + HO_2^-(aq) + H^+(aq)$$
$$HO_2(aq) + O_2^-(aq) \rightarrow O_2(aq) + HO_2^-(aq)$$

The computational tactic employed in this section follows closely that reported in our earlier studies involving $NO_2^-(aq)$ oxidation, in which case, nitrogen dioxide, NO_2, the resulting product, undergoes dismutation regenerating $NO_2^-(aq)$ [10]. Specifically, COMSOL was used to solve the governing set of coupled differential equations (see Eqs. A1 and A2, Table A.1 in dimensionless variables. The latter are defined in Table A.2) in a suitably sized axisymmetric domain, subject to the appropriate boundary conditions (see Eqs. A4-A8, Table A.1), using parameters values found in the literature (see Table A.3). As in our prior study, it will be assumed in this case, that the reduction of O_2(aq) at the disk proceeds under diffusion limited control, so as to generate a maximum amount of O_2^-(aq). Under such conditions, and given that the homogeneous disproportionation of O_2^-(aq) is second order in O_2^-(aq), its rate of disappearance would, therefore, be enhanced. In fact, it is this factor that makes it virtually impossible to prepare a O_2^-(aq) solution by dissolving a O_2^- salt, as the initially very high concentration is sufficient to generate copious amounts of oxygen. In particular, addition of solid KO_2 to ice-chilled 10 M NaOH was found to produce violent fizzing, yielding, as determined by UV-Vis spectroscopy, essentially a peroxide solution. Furthermore, the simulations will assume that the ring oxidizes O_2^-(aq) under diffusion limited conditions.

Table A.2
Definitions of Dimensionless Quantities and Parameters

Symbol	Dimensionless Variables and Parameters	Definition
P	O_2 Concentration	$\frac{[O_2]}{[O_2]_{bulk}}$
Q	O_2^- Concentration	$\frac{[O_2^-]}{[O_2]_{bulk}}$
χ	Diffusion Coefficient Ratio	$\frac{D_{O_2^-}}{D_{O_2}} = 0.372$
Z	Axial Distance from RRDE Surface	$\left(\frac{a\upsilon}{3D_{O_2}}\right)^{1/3}\left(\frac{\omega}{\upsilon}\right)^{1/2} z$
R	Radial Distance from Disk Center	$\left(\frac{a\upsilon}{3D_{O_2}}\right)^{1/3}\left(\frac{\omega}{\upsilon}\right)^{1/2} r$
Δ	Diffusion Boundary Layer Thickness	$1/J_0$
α	Rate Constant for Homogeneous O_2^-(aq) Disproportionation	$\frac{k_D[O_2]_{bulk}}{(a\upsilon/3D_{O_2})^{2/3}(D_{O_2}\omega/\upsilon)}$
J_o	Limiting Disk Current Density Assuming $\alpha = 0$	$\frac{3}{\Gamma(1/3)} \approx 1.1198$
J	Disk Current	$\left(\frac{1}{J_0\pi {R_1}^2}\right)\int_0^{R_1} 2\pi\frac{dP}{dZ}RdR$
J_{ring}	Ring Current	$\left(\frac{1}{J_0\pi {R_1}^2}\right)\int_{R_2}^{R_3} 2\pi\chi\frac{dQ}{dZ}RdR$

The correct implementation of the problem in COMSOL was validated by calculating the collection efficiency, N, of the RRDE employed assuming no dismutation, yielding a value within 0.3% of that based on the geometry of the electrode assembly.

Table A.3
List of Symbols and Their Meaning and Values

Symbol	Definition
z	Axial distance from RRDE surface
r	Radial distance from disk center
k_D	Second order homogeneous O_2^-(aq) dismutation rate constant. $k_{D,\,pH=13} = 0.499$ mol^{-1} s^{-1} [11].
D_{o_2}	Diffusion Coefficient of O_2(aq), 1.8×10^{-5} cm^2/s [12].
$D_{o_2^-}$	Diffusion Coefficient of O_2^-(aq), 6.7×10^{-6} cm^2/s [13].
$[O_2]_{bulk}$	Bulk Concentration of O_2(aq), 1.2 mM.[12]
ω	Rotation rate of the disk, 900 rpm
ν	Kinematic Viscosity, 0.01 cm^2/s
r_1	Disk radius, 0.25 cm.
r_2	Ring inner radius, 0.325 cm.
r_3	Ring outer radius, 0.375 cm.

Shown in the Upper Panel, Fig. A1 is a plot of $[O_2^-]_{surf}/\ [O_2^-]_{surf}^{\alpha=0}$ where $[O_2^-]_{surf}$ represents the concentration of (total) O_2^-(aq), i.e. $[O_2^-] + [HO_2]$, at the surface of the disk of the RRDE, assuming $\alpha \geq 0$, over that for $\alpha = 0$, i.e. no dismutation, as a function of log α, determined from the solution of the coupled differential equations above, and the parameter values specified in Table A.2. As clearly evident from the resulting curve, $[O_2^-]_{surf}/[O_2^-]_{surf}^{\alpha=0}$ is very close to one for very small values of α, which indicates that the homogeneous dismutation of $[O_2^-]$(aq) is too slow to affect its steady state value at the disk surface. As log α reaches ca. -2, $[O_2^-]_{surf}/\ [O_2^-]_{surf}^{\alpha=0}$ decreases to reach virtually 0 for log α ca. 3. The same behavior was found for plots of the ring current normalized by the collection efficiency of the RRDE, i.e. J_{ring}/N vs log α (see Lower Panel in this figure), where the ratio becomes virtually 1 (no effects due to dismutation) for log $\alpha < -2$. Since, for the conditions of our experiments (pH = 13, ω = 900 rpm) log $\alpha = -6.77$, it can be ascertained that the effects due to O_2^-(aq) dismutation are indeed negligible.

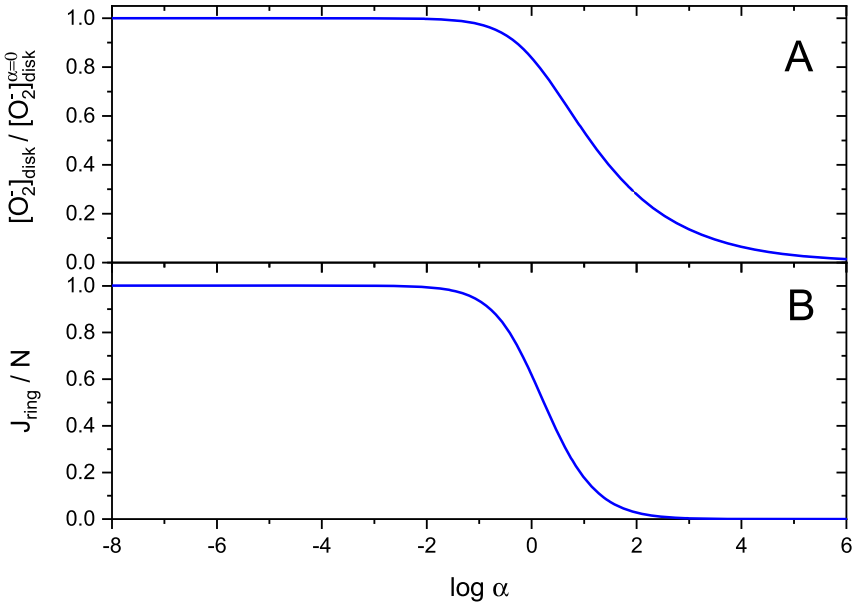

Fig. A1. Panel A. Plot of the ratio of the concentration of (total) superoxide, i.e. $[O_2^-] + [HO_2]$at the surface of the disk of the RRDE rotating at $\omega = 900$ rpm, assuming $\alpha \geq 0$, over that for $\alpha = 0$, i.e. no dismutation, as a function of log α, determined from the solution of the coupled differential equations in Table A.1, and the parameter values specified in Table A.2. **Panel B.** Dimensionless ring current, J_{ring} normalized by the collection efficiency, N, as a function of log α. The ordinate represents the fraction of solution phase superoxide that survives transit from the disk to ring electrode. Virtually identical results were obtained for $\omega = 100$ rpm and 1600 rpm.

References

[1] M.S. Hossain, D. Tryk, E. Yeager, The electrochemistry of graphite and modified graphite surfaces - the reduction of O_2-, Electrochim. Acta 34 (12) (1989) 1733–1737.

[2] K. Tammeveski, K. Kontturi, R.J. Nichols, R.J. Potter, D.J. Schiffrin, Surface redox catalysis for O-2 reduction on quinone-modified glassy carbon electrodes, J. Electroanal. Chem. 515 (1–2) (2001) 101–112.

[3] H.H. Yang, R.L. McCreery, Elucidation of the mechanism of dioxygen reduction on metal-free carbon electrodes, J. Electrochem. Soc. 147 (9) (2000) 3420–3428.

[4] H.Z. Zhang, C.H. Lin, L. Sepunaru, C. Batchelor-McAuley, R.G. Compton, Oxygen reduction in alkaline solution at glassy carbon surfaces and the role of adsorbed intermediates, J. Electroanal. Chem. 799 (2017) 53–60.

[5] R.W. Zurilla, R.K. Sen, E. Yeager, Kinetics of oxygen reduction reaction on gold in alkaline-solution, J. Electrochem. Soc. 125 (7) (1978) 1103–1109.

[6] J. Xu, W.H. Huang, R.L. McCreery, Isotope and surface preparation effects on alkaline dioxygen reduction at carbon electrodes, J. Electroanal. Chem. 410 (2) (1996) 235–242.

[7] Z. Feng, N.S. Georgescu, D.A. Scherson, Rotating ring-disk electrode method for the detection of solution phase superoxide as a reaction intermediate of oxygen reduction in neutral aqueous solutions, Anal. Chem. 88 (2) (2016) 1088–1091.

[8] I. Fromondi, A.L. Cudero, J. Feliu, D.A. Scherson, In situ UV-visible reflectance spectroscopy on single crystal Pt(111) microfacets, Electrochem. Solid State Lett. 8 (1) (2005) E9–E11.

[9] C.Z. Zhang, F.R.F. Fan, A.J. Bard, Electrochemistry of oxygen in concentrated NaOH solutions: solubility, diffusion coefficients, and superoxide formation, J. Am. Chem. Soc. 131 (1) (2009) 177–181.

[10] X.K. Xing, D.A. Scherson, Electrochemical oxidation of nitrite on a rotating gold disk electrode - a 2nd-order homogeneous disproportionation process, Anal. Chem. 60 (14) (1988) 1468–1472.

[11] B.H.J. Bielski, A.O. Allen, Mechanism of disproportionation of superoxide radicals, J. Phys. Chem. 81 (11) (1977) 1048–1050.

[12] K.E. Gubbins, R.D. Walker, Solubility and diffusivity of oxygen in electrolytic solutions, J. Electrochem. Soc. 112 (5) (1965), 469-&.

[13] M. Zhou, Y. Yu, K.K. Hu, M.V. Mirkin, Nanoelectrochemical approach to detecting short-lived intermediates of electrocatalytic oxygen reduction, J. Am. Chem. Soc. 137 (20) (2015) 6517–6523.